Florfenicol induced renal inflammatory response and apoptosis via cell adhesion molecules signaling pathway

Xiao Wang ,* Wei Liu ,* Ying Liu,* Yulan Jiao,*,†,‡ Chang Rong,* Qi Liu,* and Wanyu Shi*,†,1

*College of Traditional Chinese Veterinary Medicine, Hebei Agricultural University, Baoding, 071001, China; †Veterinary Biotechnology Innovation Center of Hebei Province, Baoding, 071001, China; and ‡Ringpu (Baoding) Biological Pharmaceutical Co., Ltd., Baoding, 071001, China.

ABSTRACT Early use of florfenicol (**FFC**) can adversely affect the health of broilers. Our previous studies showed that FFC caused kidney injury in broilers. However, the mechanism by which FFC causes nephrotoxicity remains unclear. In order to further explore the regulatory effect of FFC on specific signal pathway in the injured kidneys and the interaction between genes and proteins in this signal pathway, the transcriptome and proteome sequencing were performed on the chick kidneys in the control group and the FFC treatment group. Then, the sequencing data were analyzed, and the screened genes and proteins were verified by real-time quantitative PCR (**qPCR**) and parallel reaction monitoring (**PRM**), respectively. The results of sequencing showed that FFC exposure altered significantly the expression levels of 657 genes and 477 proteins in chick kidneys. Among them, 9 significantly differentially expressed genes (including CD28, ICOS, BLB1, BLB2, DMB2, CLDN8, CLDN18, CLDN19, and NEGR1) and 3 significantly differentially expressed proteins (including CD28, ICOS, and CLDN8) were involved in the cell adhesion molecules signaling pathway. Further analysis found that, the changes of the above genes and proteins were related to inflammation and apoptosis of the tissues and histiocytes in chick kidneys. Therefore, the structure and morphology of renal tissues, the expression levels of inflammatory and apoptotic factors, and the apoptotic rate of renal histocytes were detected. It was found that compared with the control group, there was obvious inflammatory cell infiltration in renal tissues of the FFC treatment group. At the same time, the levels of pro-inflammatory factors and pro-apoptotic factors raised significantly, and the apoptotic rate of renal histocytes increased significantly. The above results confirmed that FFC induced inflammatory reaction and apoptosis in chick kidneys by activating the cell adhesion molecules signaling pathway.

Key words: florfenicol, chick kidney, cell adhesion molecules signaling pathway, inflammation, apoptosis

2022 Poultry Science 101:102152
https://doi.org/10.1016/j.psj.2022.102152

INTRODUCTION

Florfenicol (**FFC**), a monofluorinated derivative of thiamphenicol, is a broad-spectrum veterinary antibiotic that can effectively inhibit gram-positive and gram-negative bacteria. It plays an antibacterial role mainly by interfering with the process of protein synthesis in bacteria (Arslan et al., 2021). Nowadays, FFC, as a new amide alcohol antibacterial drug instead of chloramphenicol, has been widely used in the prevention and treatment of bacterial diseases in livestock and poultry industries (Hassanin et al., 2014; Chen et al., 2016).

In recent years, the toxic and side effects of FFC on broilers had been gradually reported. One study showed that feeding hens with a 50 mg/kg FFC diet inhibited embryo growth, affected normal heart development at 4 or 5 d of age and leaded to the death of some embryos, which reduced the hatchability of chicks and increased the proportion of weak chicks hatched (Hu et al., 2020). Mei et al. (2021) found that, FFC administration increased significantly the loads of S. Enteritidis in cecal contents, spleens, and livers, as well as prolonged the residence of *S. Enteritidis*. Oral administration of FFC also altered microbiota and metabolome, thereby reducing intestinal colonization resistance and increasing susceptibility to Salmonella infection in chickens. Moreover, FFC appeared to be toxic to the developing chick embryo at around day 5 of incubation, in the absence of related toxicity in the hen and cockerel (Al-Shahrani and Naidoo, 2015).

A study showed that, the distribution and concentration of FFC in the kidneys and lungs of the treated animals

Received June 9, 2022.
Accepted August 15, 2022.

[1]Corresponding author: shiwanyu2010@126.com

were relatively high (Afifi and ElSooud, 1997). As important metabolic sites and excretory pathways of antibiotics such as FFC, kidneys of broilers are very vulnerable to its toxic and side effects. Once the kidneys of broilers are damaged by excessive FFC, their development will be seriously hindered (Wang et al., 2022). Previous studies found that FFC caused oxidative stress response in kidneys of chicks by inhibiting the expression of related factors in Nrf2-ARE pathway, and increased the apoptotic rate of renal histocytes by upregulating the expression of pro-apoptotic factors (Wang et al., 2021b; Lu et al., 2022). However, the effects of FFC on broiler kidneys are multifaceted, and its mechanisms are not completely clear. Therefore, it needs to be further studied.

Transcriptome and proteome sequencing are effective methods to explore molecular mechanisms of adverse reactions on organisms. The data at transcription level revealed that immunosuppression participated in complement activation-mediated inflammatory damage in carp gills after 4-OP treatment (Sun et al., 2022). Both of transcriptomic and proteomic data showed that prenatal BPA exposure led to the disruption of cell cycle, lipid homeostasis, and hormone balance in offspring of Wistar rats (Nguyen et al., 2020). Inflammation and apoptosis are the mechanisms that cause tissues and organs damage in animals. Han et al. (2020) found that NH_3 exposure negatively affected meat yield; and miR-6615/Smad7 axis and immune imbalance participated in NH_3-induced inflammatory injury via the NF-κB pathway inbroiler kidneys. Zhang et al. (2022) found that HSPs-triggered immunosuppression led to apoptosis of chicken peripheral blood lymphocytes under ammonia exposure.

In view of the research status of FFC and many problems exposed in its clinical application in broiler farming, chicks were taken as the research objects and given 0.15 g/L (the dosage recommended for clinical use in the instructions) FFC for continuous application in this study. Then, the chick kidneys were sequenced using transcriptome and proteome techniques to further explore the regulatory effect of FFC on specific signal pathway in the injured kidneys and the interaction between differential genes and proteins in this signal pathway. Finally, the inflammatory and apoptotic factors associated with significantly different signaling pathway in the chick kidneys were detected. The results of this study will provide experimental basis for elaborating the nephrotoxicity of FFC on broilers, and provide reasonable suggestions for its clinical application in broiler breeding, which is of great significance to promote the sustainable development of broiler breeding industry.

MATERIALS AND METHODS

Drugs and Reagents

Commercial FFC solution (clinical over-the-counter veterinary medicine, purity ≥10%) were purchased from Shenniu Biological Technical Co., Ltd. (Dezhou, China).

Total RNA extraction kit was purchased from Promega Biotechnology Co., Ltd. (Beijing, China). PrimeScript RT reagent Kit with gDNA Eraser (Perfect Real Time) and SYBR Premix Dimer Eraser reagent Kit (Perfect Real Time) were purchased from Takara Biotechnology Co., Ltd. (Dalian, China). Hematoxylin and eosin dyes were purchased from Biotopped life sciences Co., Ltd. (Beijing, China). ELISA kits of IL-1β, IL-2, TNF-α, IFN-γ, and CXCL-10 were purchased from Shanghai Enzyme-linked Biotechnology Co., Ltd. (Shanghai, China). In Situ Cell Death Detection Kit (POD) was purchased from Roche Diagnostics Co., Ltd. (Mannheim, Germany).

Animals and Experimental Design

Sixty healthy 1-day-old AA broilers were purchased from a commercial chicken farm (Hebei Dawu Agriculture and Animal Husbandry Group Poultry Co., Ltd., Baoding, China). During the experiment, chicks were kept in standard chicken houses and provided with sufficient drinking water and feed. The chicks were randomly divided into the control group and the FFC treatment group, with 3 replicates in each group, and 10 chicks in each replicate. The chicks in the control group were given tap water, and the chicks in the FFC treatment group were given tap water containing 0.15 g/L FFC recommended for clinical use in the instructions. Both groups were given standard feed. The drug was administered continuously for 5 d (the time of administration recommended in the instructions) from the first day of the experiment. On the 6th day, the drug was stopped, and 1 chick was randomly selected from each repetition of each group, that is, 3 chicks were selected from each group. Blood was collected from the vein under the wings, and sodium pentobarbital was injected intraperitoneally for euthanasia. Fresh kidney tissues were aseptically extracted and placed in enzyme-free tube for transcriptome and proteome sequencing. Three kidney tissues from the control group were labeled as KA1, KA2, and KA3, respectively. Three kidney tissues from the FFC treatment group were labeled as KB1, KB2, and KB3, respectively. Then 15 chicks were randomly selected from each group, and their kidneys were quickly removed. Part of the kidney tissues were soaked in 4% formaldehyde solution, and the rest of the kidney tissues were wrapped in tin foil and stored in a −80°C ultra-low temperature refrigerator for testing indexes.

The standard feed used in the experiment was purchased from Hebei Dawu Agriculture and Animal Husbandry Group Poultry Co., Ltd. (Baoding, China), and the transcriptome and proteome sequencing were completed by PERSONAL Company (Nanjing, China). All experimental procedures were approved by the Animal Protection and Use Committee of Hebei Agricultural University. All methods of using animals in this study were carried out in accordance with the relevant guidelines and regulations of the Animal Protection and Use Committee of Hebei Agricultural University (Baoding, China) (license No.: AUH-2021259).

Transcriptome and Proteome Sequencing

Transcriptome sequencing was performed using eukaryotic reference transcriptome assay techniques. The experimental process included total RNA extraction, total RNA quality detection, mRNA purification, mRNA fragmentation, cDNA synthesis, PCR enrichment library fragments, library quality detection, and Illumina sequencing. The differences of gene expression levels were analyzed. The conditions for screening differentially expressed genes were: the expression difference multiple $|\log_2\text{Fold change}| > 1$, and P value < 0.05.

Proteome sequencing was performed using TMT labeled quantitative proteomics techniques. The main steps included protein extraction, reduction and alkylation, trypsinolysis, TMT labeling, SCX chromatographic classification, liquid chromatographic classification, and data collection of tandem mass spectrometry (**LC-MS/MS**). The differences of protein expression levels were analyzed. The conditions for screening differentially expressed proteins were: Ratio > 1.2 or Ratio < 0.833, and P value < 0.05.

The differentially expressed genes and proteins were classified by functional enrichment, and the significantly enriched functional categories and signal pathways were found. According to GO database, functional genes are defined as molecular function (**MF**), biological process (**BP**), and cell component (**CC**). P value was calculated using hypergeometric distribution method (the standard of significant enrichment was P value < 0.05), and GO term was found out with significant enrichment of differential genes and proteins compared with the whole genome and proteome background. Then, the differential genes were associated with differential proteins and metabolic pathways according to KEGG database, so as to clarify the differences between the FFC treatment group and the control group at the level of metabolic pathway.

Combined Analysis of Transcriptome and Proteome

First, we obtained the quantitative detection and analysis results of proteome and transcriptome, and extracted the corresponding proteins and transcripts. Then extract the differential proteins and the corresponding differential transcript relationship pairs to show the consistency of the relationship pairs. Finally, proteins and related transcripts were mapped to related metabolic pathways.

qPCR of Candidate Genes

Total RNA was extracted from chick kidney tissues with the total RNA extraction kit (Promega Biotechnology Co., Ltd.). Ultramicro spectrophotometer (GENOVA NANO, JENWAY, Bibby Scientific Co., Ltd., UK) was used to detect the purity and concentration of RNA samples at 260/280 nm to ensure that the quality of samples met the test requirements. Next, total RNA was reverse transcribed into cDNA samples. The primers of the target genes were designed and synthesized by Sangon Biotech (Shanghai) Co., Ltd. (Shanghai, China) (Table 1). Strictly follow the instructions of PrimeScript RT reagent Kit with gDNA Eraser (Perfect Real Time) and SYBR Premix Dimer Eraser reagent Kit (Perfect Real Time) (Takara Biotechnology Co., Ltd.), the Ct values of screened differential genes (including CD28, ICOS, BLB1, BLB2, DMB2, CLDN8, CLDN18, CLDN19, and NEGR1), inflammatory factor genes (including IL-1β, IL-2, TFN-α, and TFN-γ), and apoptotic factor genes (including Fas, Fas-L, and JAK) in kidneys were detected using qPCR method. β-actin was used as internal reference gene. The reaction condition of qPCR was 90°C for 30 s (pre-denaturation); 95°C for 5 s, 60°C for 20 s, 72°C for 30 s (PCR reaction); 72°C for 30 s (dissolution curve analysis), a total of 40 cyclic reactions were carried out. After the experiment, the relative expression levels of target genes mRNA in chick kidneys were calculated and analyzed using $2^{-\triangle\triangle Ct}$ method (Chen et al., 2022).

PRM of Candidate Proteins

First, lysate was added into the homogenate of chick liver tissues, and the protein solution was prepared by the steps of ultrasonic, boiling water bath and centrifugation. Then, protein was quantitatively analyzed using BCA method and treated with protease. After enzymatic hydrolysis, the peptide was desalted, lyophilized, and redissolved. The concentration of peptide was determined in OD 280. PRM quantitative analysis of target peptide was performed according to the screening results of pre-experiment. The peptide information suitable for PRM analysis was imported into the software xcalibur for PRM method setting. The 2 μg peptide was taken from each sample and 20 fmol standard peptide was added. HPLC system easynlc with nanoliter flow rate was used for chromatographic separation. PRM detection was carried out on sample respectively, and the software skyline 3.5.0 was used to perform data analysis on PRM original files.

Histopathological Analysis of Kidneys in Chicks

After fixation for 24 h, kidney tissue samples were soaked with a series of gradient concentrations of ethanol and xylene, embedded in paraffin, and sliced into 5 μm sections. The slices were stained with hematoxylin and eosin (**H&E**) and sealed with neutral gum. Finally, the pathological changes of kidney tissues were observed under high power microscope (CX31RTSF, Olympus, Tokyo, Japan).

Detection of Inflammatory Factors and Chemokines in Renal Tissues by ELISA

The kidney tissues were prepared into 10% renal tissue homogenate samples using normal saline. The

Table 1. Specific primers of candidate genes used in qPCR.

Gene name	Gene ID	Primer sequence (5′-3′)	Product length (bp)
CD28	396249	F:GTGGCAGTGACGGGACTTCTTG R:CCTTGTTCTTCTGGTGAGGTGGATG	148
ICOS	424105	F:AAAGGGCGAGAAAGGAAGGCAATC R:GTGGTGCTGGTATCTGAATGCTCTG	110
BLB1	693256	F:TGGAACAGCAACGCCGAGATTC R:GCACCGTGAAGGACTCCACAAC	94
BLB2	101747454	F:CTCGGCGTTCTTCTTCTACGGTAAG R:AGATTTGCCTGTCCAGAAACCTCAC	86
DMB2	417051	F:TGCTCTTCATTGGTGTCTACTGCTG R:GATGCTGCCTGAAGGGTAGTTGTG	92
CLDN8	427974	F:ATCAGGCAAGCCAACATCAGGATG R:GCAACCAGGAAAGCCAGGAAGG	131
CLDN18	429135	F:CTTGTCTCGTCGCTGGGTGTTG R:AGCTCCTCCACAGTCCCTGATATTG	124
CLDN19	769245	F:TCCTCTTCATCCTCTGCGGTCTG R:CGTACCTGGCGTTGATTGGAGTG	108
NEGR1	395662	F:GCCGTGCTCAGGTGTTACTTGG R:AATGCACGTCTGCTCTGCTCA	139
IL-1β	395196	F:CACTGGGCATCAAGGGCTACAAG R:GTCCAGGCGGTAGAAGATGAAGC	140
IL-2	373958	F:GCAGTGTTACCTGGGAGAAGTGG R:CCGGTGTGATTTAGACCCGTAAGAC	135
TNF-α	374125	F:CTCAGGACAGCCTATGCCAACAAG R:GGCGGTCATAGAACAGCACTACG	86
IFN-γ	396398	F:CACGACATCCTTCAGCACCTCTTC R:GTTGAGGAGGCTTTGGCGTTGG	90
Fas	395274	F:CTCTTCCACCTGCTCCTCATCATTG R:TCCCCTCTCCACAGGTAATTTCTCG	145
Fas-L	429064	F:CCTTCACCAGTGGCATTCAGTACC R:CCTCGTTGTCACAGTGCCTTCC	111
JAK	395845	F:TGGATGGATACTACCGCCTGACTG R:GATGGGTCCGTGGCATTGGTTC	107
β-action	396526	F:CCAGCCATGTATGTAGCCATCCAG R:GGTAACACCATCACCAGAGTCCATC	93

contents of IL-1β, IL-2, TFN-α, TFN-γ, and CXCL-10 in 10% renal tissue homogenate samples were determined by ELISA in strict accordance with kit instructions.

Detection of Renal Histocyte Apoptotic Rate by TUNEL

The kidney tissues of chicks fixed with 4% formaldehyde solution were prepared into paraffin sections. Then according to the instructions of In Situ Cell Death Detection Kit (POD) (Roche Diagnostics Co., Ltd.), the prepared sections were tested by dewaxing, hydration, cell permeability, adding TUNEL reaction solution, adding converter-POD reagent, DAB color, hematoxylin redyeing, and sealing. After the sealed sections were dried, sections were observed under an optical microscope (400 ×) and images were collected. Five random fields were selected from each group of sections, the percentage of positive cells (tan) in the total number of cells was calculated, and the apoptotic rate of chick kidney tissue cells was analyzed.

Statistics and Analysis

Statistical analysis was performed using SPSS 19.0 (IBM Corp., Armonk, NY). All data were expressed as mean ± standard deviation. The normal distribution of test data was detected, and then the differences among groups were compared using t test. Compared with the control group, * $P < 0.05$ meant significant difference and ** $P < 0.01$ meant extremely significant difference.

RESULTS

The Number of Significantly Differentially Expressed Genes and Proteins

Compared with the control group, 657 genes with significant differences were screened from the FFC treatment group, of which 109 genes were upregulated and 548 genes were down-regulated (Figures 1A−1C).

Early FFC exposure altered significantly the expression levels of 477 proteins in the kidneys of chicks, with 198 significantly different proteins were upregulated and 279 significantly different proteins were down-regulated (Figures 1D−1F).

GO Analysis for the Transcriptome and Proteome Combined Analysis

A total of 6,439 GO Term items were screened out from the GO enrichment results, including 4,950 items

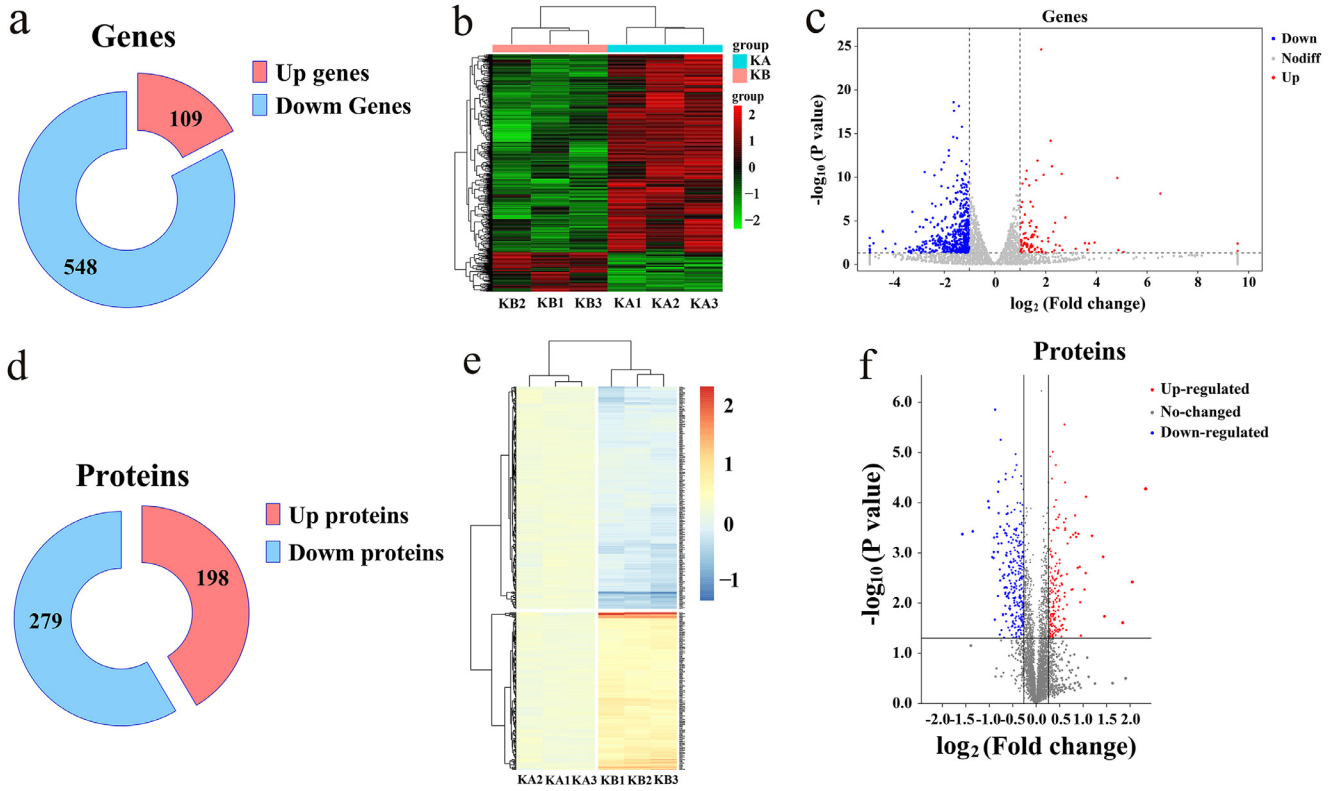

Figure 1. The significantly differentially expressed genes and proteins in chick kidneys between the FFC treatment group and the control group. (A) The number of significantly differentially expressed genes. (B) Cluster heat map of differentially expressed genes. (C) Volcano map of differentially expressed genes. (D) The number of significantly differentially expressed proteins. (E) Cluster heat map of differentially expressed proteins. (F) Volcano map of differentially expressed proteins. (In FigureC and F, the two vertical dashed lines are the thresholds for the expression of multiple of difference, the horizontal dashed line represents the threshold of significance level.)

belonging to BP, 542 items belonging to CC, and the remaining 947 items belonging to MF (Figures 2A−**2**C).

GO enrichment results showed that the differential genes and proteins were mainly enriched in BP items. The top 20 GO Term items with the smallest FDR value, namely the most significant enrichment, were selected and displayed in the bubble graph. We found that FFC modeling mainly affected the regulation of immune system process (GO: 0002682), and this item had the highest significance level in BP (Figures 2D and 2E).

KEGG Analysis for the Transcriptome and Proteome Combined Analysis

KEGG results showed 99 significantly enriched signal pathways, and the top 20 pathways with the most significant enrichment were selected for bubble diagram display. These pathways revealed the association between FFC and the biological phenomenon of renal injury. The results of bubble map showed that the top 20 typical pathways with significant enrichment of difference factors were mainly distributed in Environmental information processing, Metabolism and Cellular processes. The significantly differentially expressed factors were mainly enriched in cell adhesion molecules (**CAMs**) signaling pathway, which belonged to environmental information processing and metabolism. It was consistent with the regulation of immune system process indicated by GO enrichment results (Figures 2F and G).

The Significantly Differentially Expressed Genes and Proteins in Cell Adhesion Molecules Signaling Pathway

Results of Combined Transcriptome and Proteome Analysis The results of combined transcriptome and proteome analysis showed that compared with the control group, there were 9 significantly differentially expressed genes and 3 significantly differentially expressed proteins in the cell adhesion molecules signaling pathway of the chick kidneys treated with FFC. Among them, 3 genes with significant differences also had significant differences in corresponding proteins. Gene expression levels of CD28, ICOS, BLB1, BLB2, DMB2, CLDN8, CLDN18, CLDN19, and NEGR1 were upregulated significantly. Protein expression levels of CD28, ICOS, and CLDN8 were upregulated significantly, too. The differential genes and proteins were mapped to the cell adhesion molecules signaling pathway, and a simplified diagram containing all differential genes and proteins was constructed (Figure 3A).

Results of qPCR Verification Compared with the control group, the mRNA expression levels of CD28, ICOS, BLB1, BLB2, DMB2, CLDN8, CLDN18,

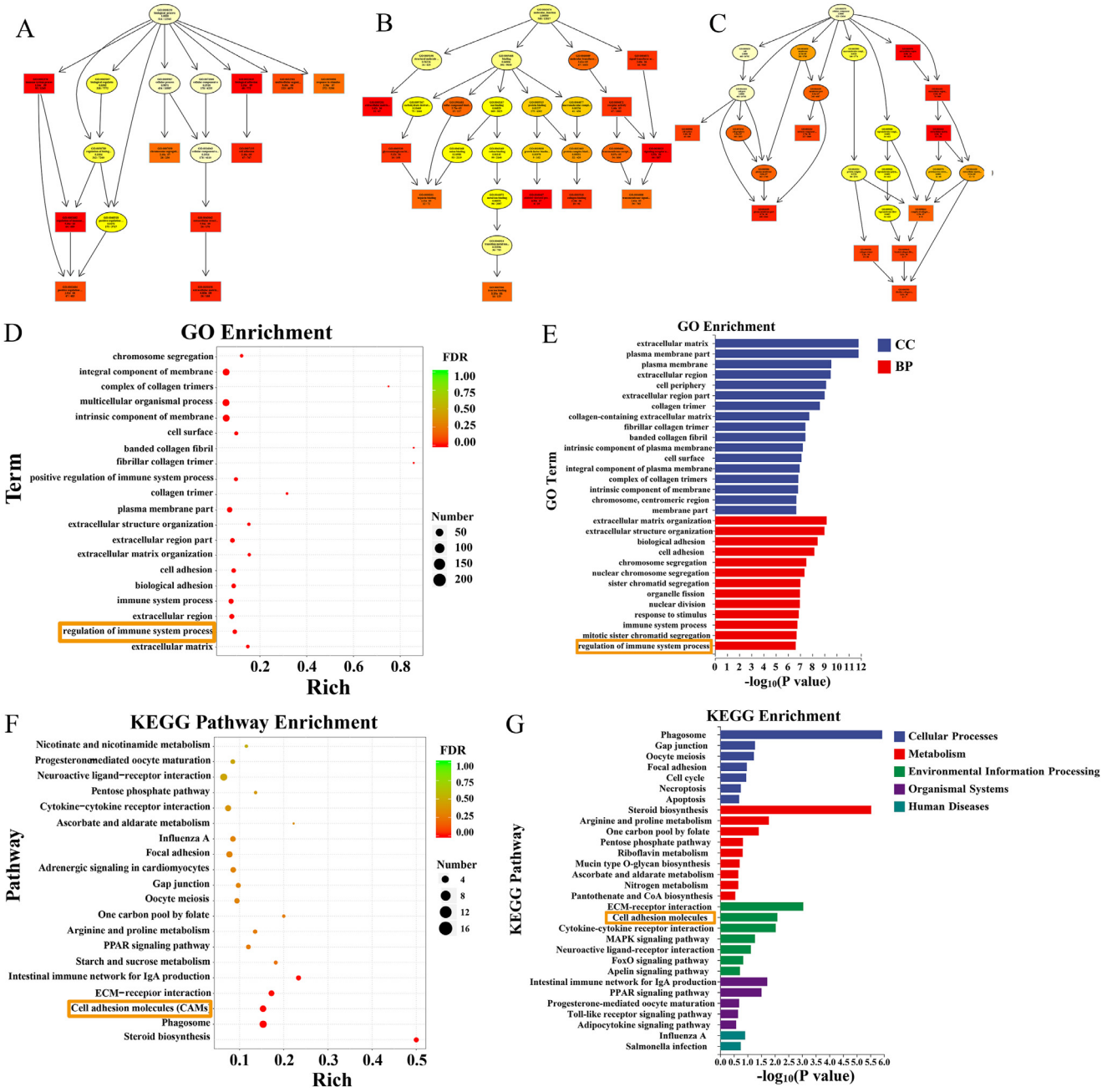

Figure 2. GO and KEGG analysis results for the transcriptome and proteome combined analysis. (A) DAG concentration diagram of biological process (BP) in GO database. (B) DAG concentration diagram of molecular function (MF) in GO database. (C) DAG concentration diagram of cellular component (CC) in GO database. (D) Bubble chart of GO enrichment results for the transcriptome and proteome combined analysis. (E) Histogram of GO enrichment results for the transcriptome and proteome combined analysis. (F) Bubble chart of KEGG enrichment results for the transcriptome and proteome combined analysis. (G) Histogram of KEGG enrichment results for the transcriptome and proteome combined analysis. (In Figure A−C, each node represents a GO term, and branches represent inclusion relations, the function range defined from top to bottom is getting smaller and smaller, the box represents the GO terms with top10 enrichment degree, and the darker the color, the higher the enrichment degree. In Figure D−G, rich factor refers to the ratio of the number of differential genes enriched to the GO term to the number of genes annotated to the GO term, the larger the Richfactor, the greater the degree of enrichment (abscissa), the value range of FDR generally ranges from 0 to 1 and the closer it is to 0, the more significant the enrichment is.)

CLDN19, and NEGR1 in the FFC treatment group were upregulated significantly. The results of qPCR were consistent with those of transcriptome, thus confirming the accuracy of transcriptome (Figures 3B and 3C).

Results of PRM Verification PRM technique was used to validate the protein expression levels of CD28, ICOS, and CLDN8, which were different significantly with more than 2 specific peptides. Compared with the control group, the expression levels of 3 proteins (including CD28, ICOS, and CLDN8) were upregulated significantly in the FFC treatment group. Since the results were secondary identification based on proteomics, PRM had a high accuracy. However, the coelution of peptides of significantly different proteins would produce quantitative ratio compression effect, resulting in lower quantitative difference than actual difference (Figures 3D and 3E).

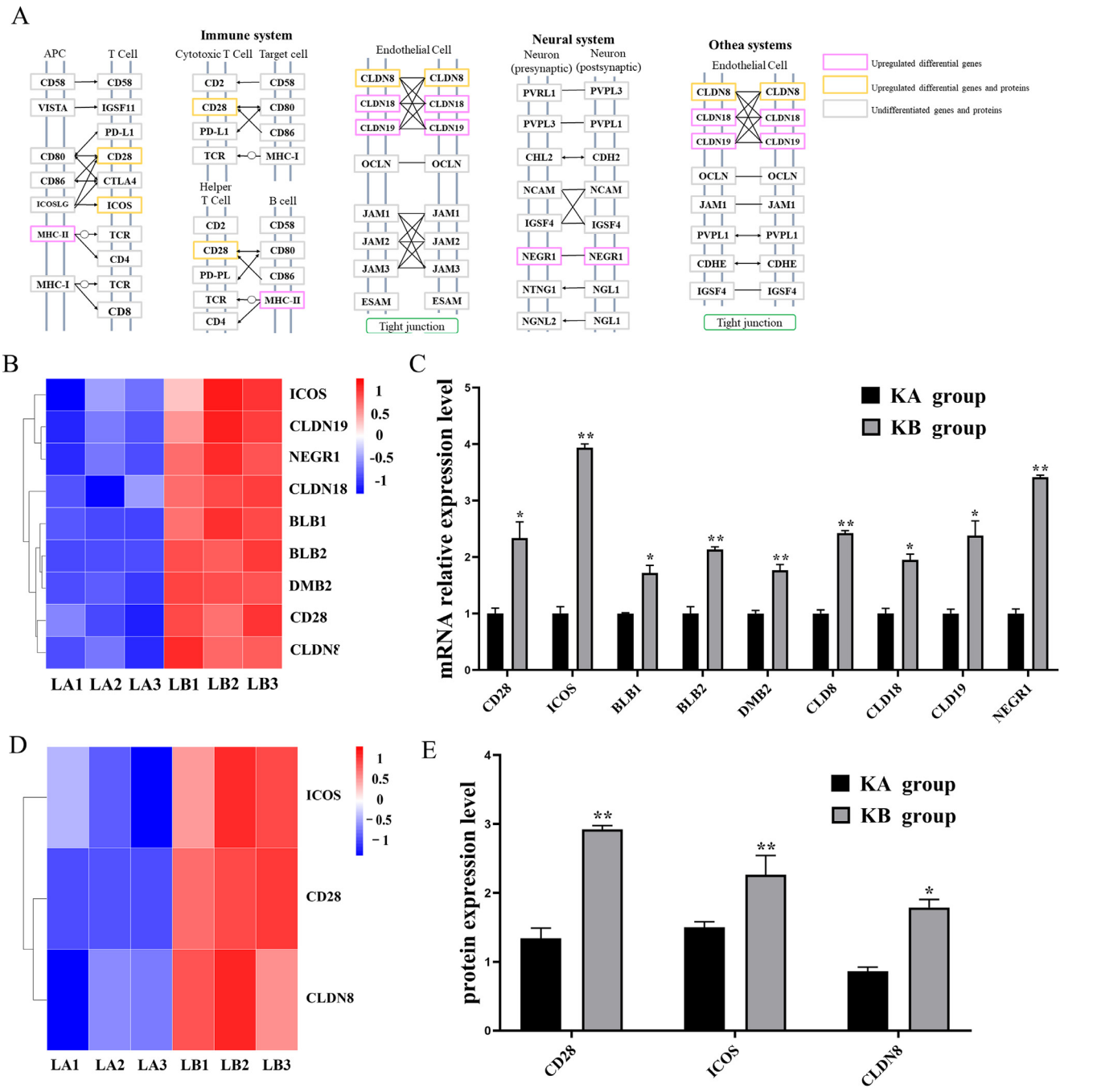

Figure 3. The significantly differentially expressed genes and proteins of cell adhesion molecules signaling pathway in chick kidneys. (A) Cell adhesion molecules signaling pathway diagram. (B) Heat maps of 9 significantly differentially expressed genes. (C) The mRNA relative expression levels of CD28, ICOS, BLB1, BLB2, DMB2, CLDN8, CLDN18, CLDN19, and NEGR1 gene. (D) Heat maps of 3 significantly differentially expressed proteins. (E) The expression levels of CD28, ICOS, and CLDN8 protein. (KA represents the control group, and KB represents the FFC treatment group. Compared with the control group, * means $P < 0.05$, ** means $P < 0.01$.)

Effect of FFC Exposure on the Histopathological Changes

In the control group, the renal tissue structure was intact, and no obvious structural damage and necrosis, no renal tissue congestion, and no inflammatory cell infiltration were observed. However, the renal structure of chicks in the FFC treatment group was abnormal, which showed that the structure of nephron was disordered, the boundary was fuzzy, epithelial cells were necrotic, a large number of inflammatory cells were accumulated in tissue space, and some renal tissues were congested (Figure 4).

Effect of FFC Exposure on Inflammatory Factors and Chemokines in Renal Tissues

Compared with the control group, FFC exposure increased significantly the mRNA relative expression levels and contents of inflammatory factors IL-1β, IL-2, TFN-α and TFN-γ in chick kidneys (Figures 5A–5H).

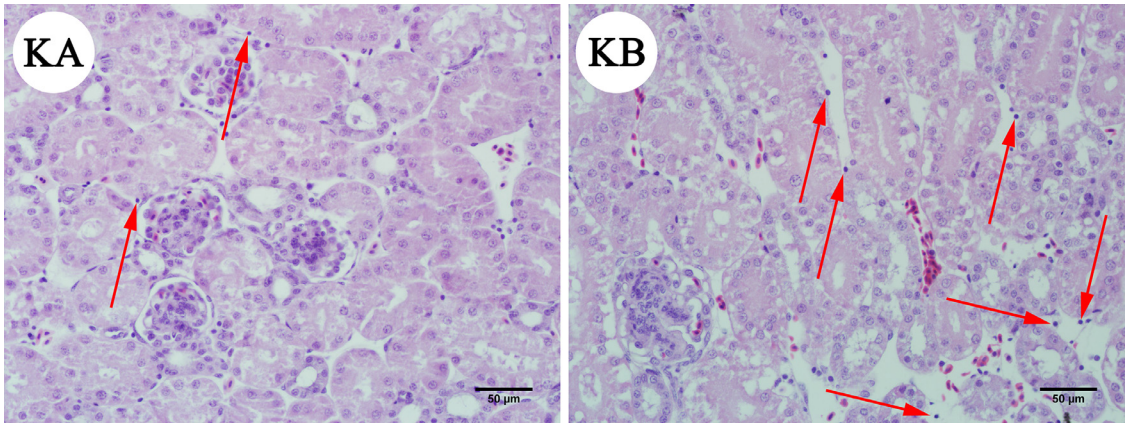

Figure 4. Structure and morphology of tissues and histocytes in chick kidneys (H&E staining, 400 ×). (KA represents the control group, and KB represents the FFC treatment group. There are inflammatory cells infiltration in chick kidneys at the red arrows.)

The content of chemokine CXCL-10 in chick kidneys of the FFC treatment group was increased significantly, too (Figure 5I).

Effect of FFC Exposure on Apoptotic Factors in Renal Tissues

Except that the level of Fas mRNA did not change significantly, the relative expression levels of Fas-L and JAK mRNA in the kidneys of chicks treated with FFC were significantly higher than those in the control group (Figures 6A–6C).

Effect of FFC Exposure on Renal Histocyte Apoptotic Rate

The number of apoptotic cells with brown nuclei in the FFC treatment group was significantly higher than that in the control group (Figure 6D). By calculation, the apoptotic rate of renal histocytes in the FFC treatment group was increased significantly (Figure 6E).

DISCUSSION

The kidney participates in the metabolism of drugs in animals and is the main excretory organ. While the kidney plays its functional role, it is extremely vulnerable to the damage of antibiotics such as FFC (Wang et al., 2021a). We added FFC to the drinking water of chicks to detect its effects on renal function. Transcriptome and proteome analysis showed that early FFC exposure changed significantly the expression of some genes (including CD28, ICOS, BLB1, BLB2, DMB2, CLDN8, CLDN18, CLDN19, and NEGR1) and proteins (including CD28, ICOS, and CLDN8) in cell adhesion molecules signaling pathway. Moreover, these differential genes and proteins were related to inflammation and apoptosis

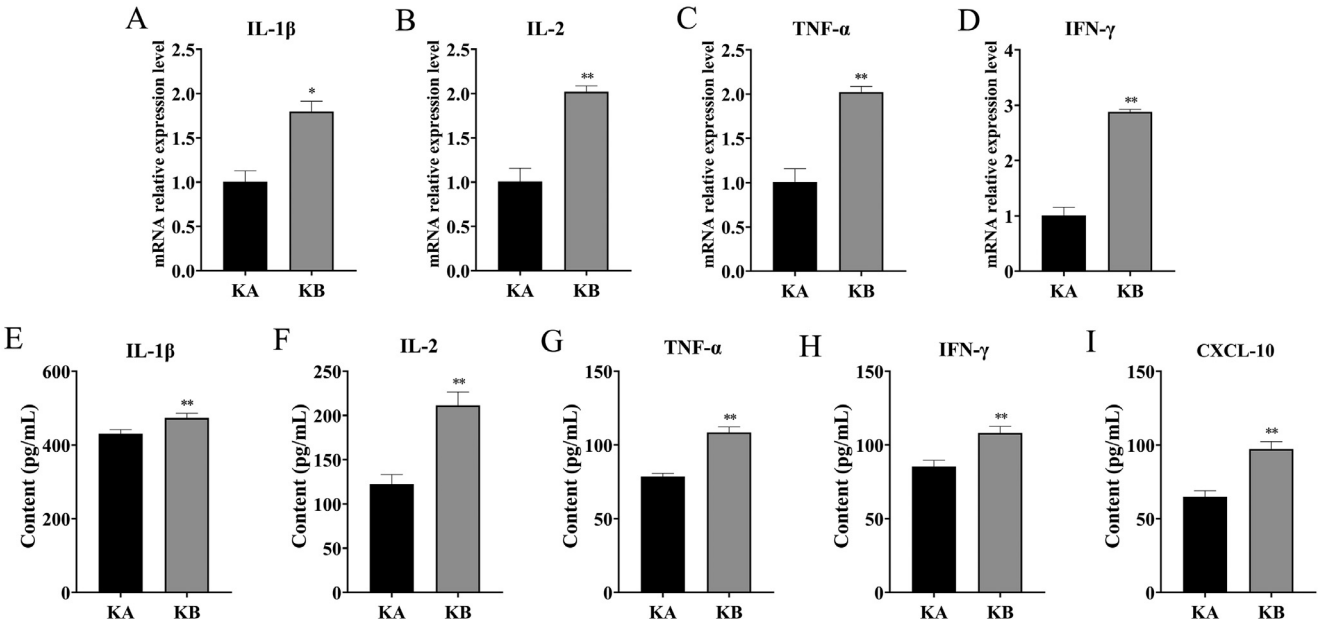

Figure 5. The levels of inflammatory factors and chemokines in renal tissues of chicks. (A) The mRNA relative expression level of IL-1β. (B) The mRNA relative expression level of IL-2. (C) The mRNA relative expression level of TFN-α. (D) The mRNA relative expression level of IFN-γ. (E) The content of IL-1β. (F) The content of IL-2. (G) The content of TFN-α. (H) The content of IFN-γ. (I) The content of CXCL-10. (KA represents the control group, and KB represents the FFC treatment group. Compared with the control group, * means $P < 0.05$, ** means $P < 0.01$.)

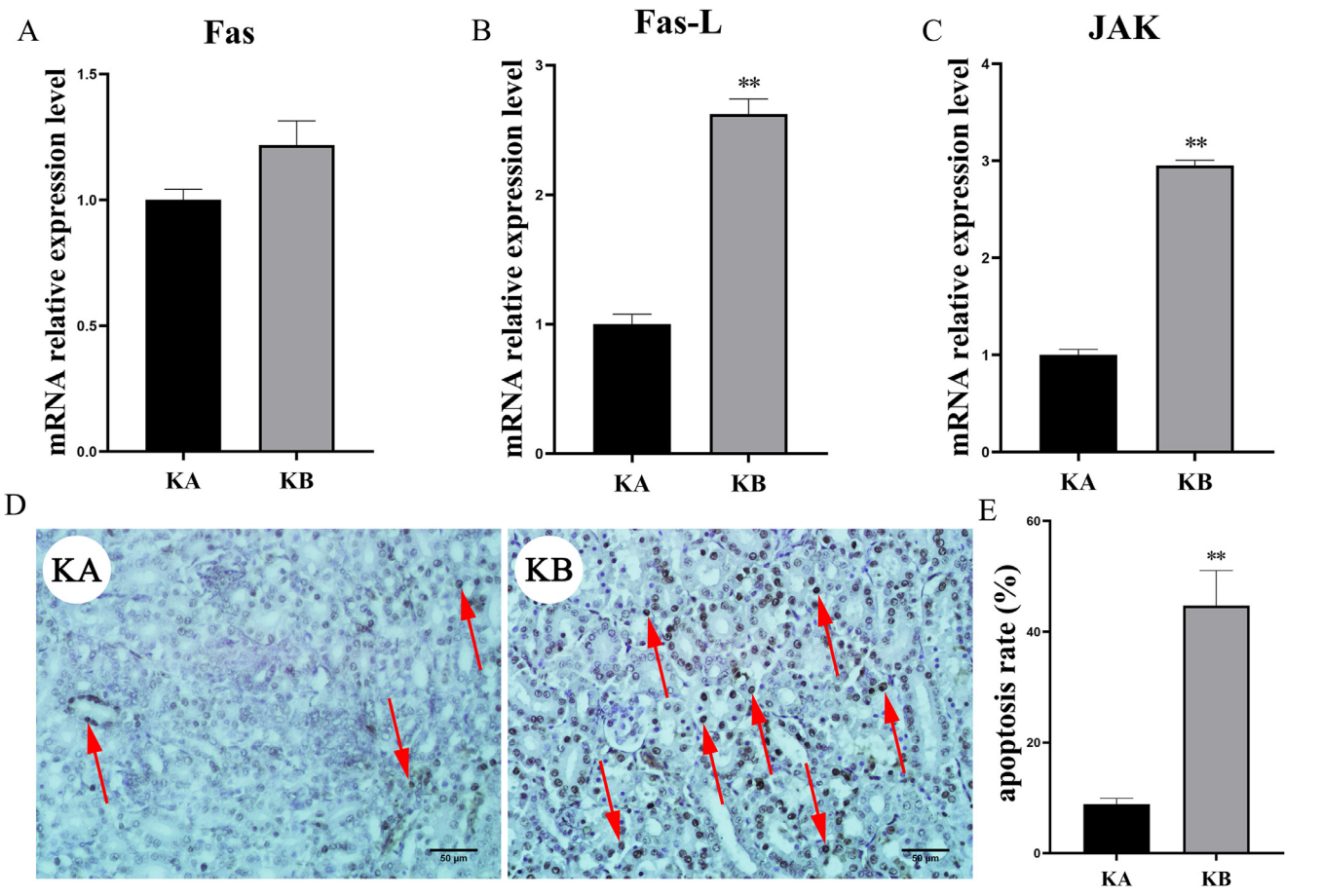

Figure 6. Apoptotic levels of renal histocytes in chicks. (A) The mRNA relative expression level of Fas. (B) The mRNA relative expression level of Fas-L. (C) The mRNA relative expression level of JAK. (D) TUNEL test results of renal histocytes. (E) Apoptotic rate of renal histocytes. (KA represents the control group, and KB represents the FFC treatment group. Compared with the control group, * means $P < 0.05$, ** means $P < 0.01$. In Figure 6D, there are apoptotic renal histocytes of chicks at the red arrows.)

in chick kidneys. CAMs mainly exist between tissues and cells, including selectins family, integrins family, cadherins family, and IgCAMs family (Hintermann and Christen, 2019). CAMs play an adhesion role by identifying specific receptors that can bind to it, which can induce the occurrence and development of pathological processes of inflammatory response and apoptosis (Harjunpää et al., 2019). These findings support our results in this study.

Sequencing and validation results showed that the expression levels of CD28 and inducible co stimulator (**ICOS**) in the kidneys of chicks exposed to FFC increased significantly. CD28 and ICOS belong to CD28 family, which are located upstream of the cell adhesion molecules signaling pathway. CD28 is a 44 ku homologous dimer glycoprotein linked by disulfide bonds. It was found to induce IL-2 secretion by upregulating IL-2 mRNA expression level (Martkamchan et al., 2016). CD28 can also promote Fas and Fas-L-mediated T cell apoptosis by binding to ligands (Tschumi et al., 2018). ICOS is a member of the newly discovered CD28 family with a relative molecular weight of 55 to 60 ku. ICOS mainly plays a role after CD28 and can regulate the activation of T cells and the secretion of cytokines (Fu et al., 2011). It also promotes T cells to produce IL-1, TFN-α, and TFN-γ, but it has no obvious effect on the production of IL-2 (Guedan et al., 2018).

Major histocompatibility complex (**MHC**) belongs to the selectin family and is the B complex of chicken. MHC class molecules are receptor polygene family, whose function is to bind and present antigenic peptides to T cells (Griffin et al., 2021). MHC-II class molecules play an important role in signal transduction in the cell adhesion molecules signaling pathway. BLBs belong to classical MHC-II class molecules, and have 2 backward complementary copy genes, BLB1 and BLB2, which have high homology (Guo et al., 2012). They are located on the surface of antigen presenting cells and participate in the antigen presenting recognition process in cellular adaptive immune response, and are crucial for the initiation of adaptive immune response (Parker and Kaufman, 2017). DMB2 belongs to non-classical MHC-II class molecules, which is located near BLBs gene. It has high conservation and the advantage of expression in multiple tissues. DMB2 can assist the classical MHC-II class molecules to complete the antigen presentation process (Chenani et al., 2021). Some scholars speculated that BLB2/DMB2 system, which was widely expressed in multiple tissues, was the main MHC-II class molecular system in chickens (Parker and Kaufman, 2017). The results of sequencing and validation showed that FFC induced a significant increase in the expression levels of BLB1, BLB2, and DMB2 in chick kidneys, that is, it increased significantly the expression levels of classical

and non-classical MHC-II class molecules. One other study showed that MHC-Ⅱ class molecules were related to the immune response mechanism of chicks, and the over-activation of this mechanism could make MHC-II class molecules excited to present exogenous antigens, promote the proliferation of B cells and the expression of inflammatory factors, and easily induce the body to produce abnormal immune response (Eren et al., 2022). Therefore, we speculated that FFC might induce chick kidney inflammation through this mechanism.

The main feature of inflammatory reaction in kidneys is that a large number of inflammatory cells transfer from various parts of the animal body to the kidney, and then release various inflammatory factors (Yao et al., 2021). C-X-C motif chemokine ligand 10 (**CXCL-10**) is an important chemokine, and can induce the activation of T lymphocytes and natural killer cells (**NK cells**) (Calabriso et al., 2020). CXCL-10 can migrate activated T lymphocytes and NK cells to the sites of inflammation, cause the formation of inflammatory microenvironments, and lead to immune or inflammatory responses in the acute stage (Chenani et al., 2021). We found that the expression level of CXCL-10 in the kidneys increased after the addition of FFC to the drinking water of chicks. At the same time, histopathological sections showed that a large number of inflammatory cells gathered in renal tissues. This may be related to the overexpression of CXCL-10.

The claudins (**CLDN**) family of cell adhesion molecules signaling pathway can participate in inflammatory reaction together with CXCL-10. CLDN family mainly plays an important role in controlling cell permeability and maintaining tissue homeostasis (Liu et al., 2017). CLDN8 is mainly expressed in endothelial cells, and is highly expressed in renal tissues, with tightly connected physiological functions (Liu et al., 2019). CLDN18, CLDN19, and CLDN8 all belong to the CLDN family, which are the skeleton proteins that can connect cells and maintain the dynamic balance between cells (Li et al., 2020). Transcriptome and proteome sequencing results showed that the expression levels of CLDN8, CLDN18, and CLDN19 in the kidneys of chicks were upregulated after treatment with FFC. The inflammatory cells might be attracted to the injury sites of kidneys by CXCL10, and then connected with renal tissue cells under the action of CLDN8, CLDN18, and CLDN19. Then, the inflammatory cells gathered in the renal tissues synthesized and secreted pro-inflammatory factors, triggering inflammatory response.

The infiltration of inflammatory cells is an important manifestation of animal kidney injury. The expression levels of inflammatory factors are closely related to the severity of immune injury in animal kidneys, and play an important role in cell adhesion molecules signaling pathway (Huang et al., 2021). Due to the underdevelopment of renal function of chicks, infiltration of inflammatory cells was easy to cause inflammatory reaction in kidneys. Therefore, we detected the contents of 4 common pro-inflammatory factors, IL-1β, IL-2, TFN-α, and TFN-γ, which are downstream factors in the cell adhesion molecules signaling pathway in chick kidneys. It was found that the contents of the 4 pro-inflammatory factors were increased significantly in the kidneys of FFC-treated chicks. Huang et al. (2021) found that excessive lead induced inflammatory damage in chicken kidneys by increasing the expression levels of IL-1β and TNF-α. Wang et al. (2018a) found that cadmium increased significantly the levels of inflammatory factors in chicken kidney tissues and caused the occurrence of inflammatory response. The mechanism of lead and cadmium induced nephritis injury in chickens in the above studies is similar to the mechanism of FFC induced inflammatory response in chick kidneys in present study.

FFC exposure induced the high expression of CD28, ICOS, MHC-II class molecules, and CLDNs, increased the secretion of pro-inflammatory factors such as IL-1β, IL-2, TFN-α, TFN-γ, and CXCL-10, and caused the generation and expansion of inflammation in the kidneys of chicks. Other studies found that the increase of inflammatory factors such as IL-1β, IL-2, and TFN-γ could in turn promote the expression of MHC-II class molecules, thus aggravating the inflammatory response in the kidneys of chicks (Singh et al., 2018).

Intense inflammatory reaction can increase the number of apoptotic cells and accelerate the rate of apoptosis (Gao et al., 2017). The dynamic balance between apoptosis and proliferation is the basic process necessary to maintain the homeostasis of animal body (Bertheloot et al., 2021). However, excessive apoptosis of tissue cells will lead to dysfunction. Excessive apoptosis caused renal dysfunction in chicks, which further damaged the kidney (Wang et al., 2018b,c). The increase of CD28 expression could also activate Fas/Fas-L-mediated apoptosis pathways, leading to excessive apoptosis of chicken kidney tissue cells (Jones et al., 2002). Fas/Fas-L system is one of the main forms of death receptor system that mediate histocytes apoptosis (Su et al., 2020; Yu et al., 2020). We detected the expression levels of Fas and Fas-L mRNA. The results showed that there was no significant difference in the expression of Fas between the control group and the FFC treatment group. It further indicated that Fas was expressed in normal kidney tissues of chicks, and its expression level was not affected by FFC exposure. However, the expression level of Fas-L in the kidneys of chicks treated with FFC increased significantly. Excessive expression of Fas-L combined with its ligand Fas located on the surface of renal histocytes, resulting in apoptosis of many renal histocytes.

MiR-25-5p/NEGR1 axis regulates the JAK-STAT pathway, which is a common apoptotic pathway (Miao et al., 2022). Neuronal growth regulator 1 (**NEGR1**) consists of 7 exons and 6 introns, is a kind of glycosyl phosphatidyl inositol anchor protein. As a cell adhesion factor, NEGR1 belongs to the IgLON subgroup of the immunoglobulin superfamily and is a key gene in miR-25-5p/NEGR1 axis, which controls apoptosis of endothelial cells (Zhang et al., 2019). Sequencing and validation results showed that FFC induced the upregulation

of NEGR1 expression in kidneys of chicks, stimulated the biological function of miR-25-5p/NEGR1 axis. Then, it increased the expression of JAK, induced the activation of JAK-STAT pathway, and promoted the apoptosis process of renal histocytes.

CONCLUSIONS

In this study, the database of transcriptome and proteome was constructed and analyzed jointly, the sequencing data were deeply excavated, and the screened sequencing results were verified using qPCR and PRM. The sequencing data suggested that the early continuous application of FFC with recommended dose activated the cell adhesion molecules signaling pathway in chick kidneys and upregulated the expression levels of some factors in this signaling pathway. Under the regulation of this pathway, a large number of inflammatory cells might be adhered to the renal tissues. Next, some pro-inflammatory factors were released, which in turn induced the inflammatory response in kidneys. At the same time, the overexpression of some factors in cell adhesion molecules signal pathway induced by FFC also caused the increase of the expression levels of pro-apoptotic factors, and then promoted the apoptosis of renal histocytes.

ACKNOWLEDGMENTS

This study was supported by Key Research and Development Plan Project of Hebei Province (No. 22326622D).

DISCLOSURES

The authors declare that they have no known competing financial interests or personal relationships that could have appeared to influence the work reported in this paper.

SUPPLEMENTARY MATERIALS

Supplementary material associated with this article can be found, in the online version, at doi:10.1016/j.psj.2022.102152.

REFERENCES

Afifi, N. A., and K. A. ElSooud. 1997. Tissue concentrations and pharmacokinetics of florfenicol in broiler chickens. Br. Poult. Sci. 38:425–428.

Al-Shahrani, S., and V. Naidoo. 2015. Florfenicol induces early embryonic death in eggs collected from treated hens. BMC Vet. Res. 11:213.

Arslan, P., B. Yurdakok-Dikmen, S. C. Ozeren, O. Kuzukiran, and A. Filazi. 2021. In vitro effects of erythromycin and florfenicol on primary cell lines of Unio crassus and Cyprinus carpio. Environ. Sci. Pollut. Res. Int. 28:48408–48416.

Bertheloot, D., E. Latz, and B. S. Franklin. 2021. Necroptosis, pyroptosis and apoptosis: an intricate game of cell death. Cell. Mol. Immunol. 18:1106–1121.

Calabriso, N., M. Massaro, E. Scoditti, A. Pasqualone, B. Laddomada, and M. A. Carluccio. 2020. Phenolic extracts from whole wheat biofortified bread dampen overwhelming inflammatory response in human endothelial cells and monocytes: major role of VCAM-1 and CXCL-10. Eur. J. Nutr. 59:2603–2615.

Chen, D., J. Liang, C. Jiang, D. Wu, B. Huang, X. Teng, and Y. Tang. 2022. Mitochondrion participated in effect mechanism of manganese poisoning on heat shock protein and ultrastructure of testes in chickens [e-pub ahead of print]. Biol. Trace Elem. Res, doi:10.1007/s12011-022-03259-7.

Chen, Y., J. Sun, X. P. Liao, Y. Shao, L. Li, L. X. Fang, and Y. H. Liu. 2016. Impact of enrofloxacin and florfenicol therapy on the spread of OqxAB gene and intestinal microbiota in chickens. Vet. Microbiol. 192:1–9.

Chenani, H., M. Nazari, M. T. Beigi Nassiri, H. Roshanfekr, and A. Aghaie. 2021. Exonic SNP in MHC-DMB2 is associated with gene expression and humoral immunity in Japanese quails. Vet. Immunol. Immunopathol. 239:110302.

Eren, U., S. Kum, A. Nazligul, O. Gules, E. Aka, M. Yildiz, and S. Zorlu. 2022. TLR2 and TLR4 molecules and antigen-presenting cell compositions in cecal tonsils of broiler chicks (Gallus gallus domesticus) in the first two weeks of the post-hatch period. Anatomia, Histologia, Embryologia 51:125–135.

Fu, T., Q. He, and P. Sharma. 2011. The ICOS/ICOSL pathway is required for optimal antitumor responses mediated by anti-CTLA-4 therapy. Cancer Res 71:5445–5454.

Gao, Y., L. Ma, C. L. Luo, T. Wang, M. Y. Zhang, X. Shen, H. H. Meng, M. M. Ji, Z. F. Wang, X. P. Chen, and L. Y. Tao. 2017. IL-33 exerts neuroprotective effect in mice intracerebral hemorrhage model through suppressing inflammation/apoptotic/autophagic pathway. Mol. Neurobiol. 54:3879–3892.

Griffin, B. D., J. C. Corredor, Y. Pei, and É. Nagy. 2021. Downregulation of cell surface major histocompatibility complex class I expression is mediated by the left-end transcription unit of fowl adenovirus 9. Viruses 13:2211.

Guedan, S., A. D. Posey Jr., C. Shaw, A. Wing, T. Da, P. R. Patel, S. E. McGettigan, V. Casado-Medrano, O. U. Kawalekar, M. Uribe-Herranz, D. Song, J. J. Melenhorst, S. F. Lacey, J. Scholler, B. Keith, R. M. Young, and C. H. June. 2018. Enhancing CAR T cell persistence through ICOS and 4-1BB costimulation. JCI Insight 3:e96976.

Guo, X. L., H. Q. Zheng, X. L. Li, Y. Li, Z. L. Gu, C. S. Zheng, Z. H. Wei, J. S. Wang, R. Y. Zhou, and L. H. Li. 2012. Genetic variation of major histocompatibility complex BLB2 gene exon 2 in Hebei domestic chicken. Res. Vet. Sci. 92:76–79.

Han, Q., J. Tong, Q. Sun, X. Teng, H. Zhang, and X. Teng. 2020. The involvement of miR-6615-5p/Smad7 axis and immune imbalance in ammonia-caused inflammatory injury via NF-κB pathway in broiler kidneys. Poult. Sci. 99:5378–5388.

Harjunpää, H., M. Llort Asens, C. Guenther, and S. C. Fagerholm. 2019. Cell adhesion molecules and their roles and regulation in the immune and tumor microenvironment. Front. Immunol. 10:1078.

Hassanin, O., F. Abdallah, and A. Awad. 2014. Effects of florfenicol on the immune responses and the interferon-inducible genes in broiler chickens under the impact of E. coli infection. Vet. Res. Commun. 38:51–58.

Hintermann, E., and U. Christen. 2019. The many roles of cell adhesion molecules in hepatic fibrosis. Cells 8:1503.

Hu, D., F. Meng, Y. Cui, M. Yin, H. Ning, Z. Yin, L. Chen, Y. Ge, and S. Liu. 2020. Growth and cardiovascular development are repressed by florfenicol exposure in early chicken embryos. Poult. Sci. 99:2736–2745.

Huang, H., J. Q. Chen, Q. Sun, Y. H. Liu, Y. Tang, and X. H. Teng. 2021. NLRP3 inflammasome is involved in the mechanism of mitigative effect of selenium on lead-induced inflammatory damage in chicken kidneys. Environ. Sci. Pollut. R 28:10898–10908.

Jones, R. G., A. R. Elford, M. J. Parsons, L. Wu, C. M. Krawczyk, W. C. Yeh, R. Hakem, R. Rottapel, J. R. Woodgett, and P. S. Ohashi. 2002. CD28-dependent activation of protein kinase B/Akt blocks Fas-mediated apoptosis by preventing death-inducing signaling complex assembly. J. Exp. Med. 196:335–348.

Li, J., Y. Zhang, D. Hu, T. Gong, R. Xu, and J. Gao. 2020. Analysis of the expression and genetic alteration of CLDN18 in gastric cancer. Aging 12:14271–14284.

Liu, B., B. Lu, X. Wang, H. Jiang, and W. Kuang. 2019. MiR-361-5p inhibits cell proliferation and induces cell apoptosis in retinoblastoma by negatively regulating CLDN8. Childs Nerv. Syst. 35:1303–1311.

Liu, T. H., R. H. Chung, S. C. Wang, C. P. Fang, H. H. Tsou, C. L. Shih, H. W. Kuo, Y. Wang, and Y. L. Liu. 2017. Missense mutation at CLDN8 associated with a high plasma interferon gamma-inducible protein 10 level in methadone-maintained patients with urine test positive for morphine. PLoS One 12:e0187639.

Lu, C., L. Zhang, Y. Cui, G. Jin, Y. Bao, and W. Shi. 2022. Proteome and transcriptome explore the mechanism of Salvia miltiorrhiza polysaccharides to relieve florfenicol-induced kidney injury in broilers. Environ. Sci. Pollut. Res. Int 29:45872–45884.

Martkamchan, S., N. Onlamoon, S. Wang, K. Pattanapanyasat, and P. Ammaranond. 2016. The effects of anti-CD3/CD28 coated beads and IL-2 on expanded T cell for immunotherapy. Adv. Clin. Exp. Med. 25:821–828.

Mei, X., B. Ma, X. Zhai, A. Zhang, C. Lei, L. Zuo, X. Yang, C. Zhou, and H. Wang. 2021. Florfenicol enhances colonization of a Salmonella enterica serovar enteritidis floR mutant with major alterations to the intestinal microbiota and metabolome in neonatal chickens. Appl. Environ. Microbiol. 87:e0168121.

Miao, Y., D. Niu, Z. Wang, J. Wang, Z. Wu, J. Bao, W. Hu, Y. Guo, R. Li, M. Ishfaq, and J. Li. 2022. Mycoplasma gallisepticum induced inflammation-mediated Th1/Th2 immune imbalance via JAK/STAT signaling pathway in chicken trachea: Involvement of respiratory microbiota. Vet. Microbiol. 265:109330.

Nguyen, H. T., K. Yamamoto, M. Iida, T. Agusa, M. Ochiai, J. Guo, R. Karthikraj, K. Kannan, E. Y. Kim, and H. Iwata. 2020. Effects of prenatal bisphenol A exposure on the hepatic transcriptome and proteome in rat offspring. Sci. Total Environ. 720:137568.

Parker, A., and J. Kaufman. 2017. What chickens might tell us about the MHC class II system. Curr. Opin. Immunol. 46:23–29.

Singh, M. K., F. Jamal, A. K. Dubey, P. Shivam, S. Kumari, G. Ahmed Pushpanjali, M. R. Dikhit, S. Narayan, V. N. R. Das, K. Pandey, K. K. Sinha, P. Das, and S. K. Singh. 2018. Co-factor-independent phosphoglycerate mutase of Leishmania donovani modulates macrophage signalling and promotes T-cell repertoires bearing epitopes for both MHC-I and MHC-II. Parasitology 145:292–306.

Su, C. M., Y. S. Weng, L. Y. Kuan, J. H. Chen, and F. T. Hsu. 2020. Suppression of PKCδ/NF-κB signaling and apoptosis induction through extrinsic/intrinsic pathways are associated magnolol-inhibited tumor progression in colorectal cancer in vitro and in vivo. Int. J. Mol. Sci. 21:3527.

Sun, Q., Y. Liu, X. Teng, P. Luan, X. Teng, and X. Yin. 2022. Immunosuppression participated in complement activation-mediated inflammatory injury caused by 4-octylphenol via TLR7/IκBα/NF-κB pathway in common carp (Cyprinus carpio) gills. Aquat. Toxicol. (Amsterdam, Netherlands) 249:106211.

Tschumi, B. O., N. Dumauthioz, B. Marti, L. Zhang, E. Lanitis, M. Irving, P. Schneider, J. P. Mach, G. Coukos, P. Romero, and A. Donda. 2018. CART cells are prone to Fas- and DR5-mediated cell death. J. Immunother. Cancer 6:71.

Wang, X., R. Bao, and J. Fu. 2018a. The antagonistic effect of selenium on cadmium-induced damage and mRNA levels of selenoprotein genes and inflammatory factors in chicken kidney tissue. Biol. Trace Elem. Res. 181:331–339.

Wang, X., C. Han, Y. Cui, S. Li, G. Jin, W. Shi, and Y. Bao. 2021a. Florfenicol causes excessive lipid peroxidation and apoptosis induced renal injury in broilers. Ecotoxicol. Environ. Saf. 207:111282.

Wang, X., C. Han, Y. Q. Cui, Y. M. Geng, Y. Y. Wei, W. Y. Shi, and Y. Z. Bao. 2021b. Florfenicol induces renal toxicity in chicks by promoting oxidative stress and apoptosis. Environ. Sci. Pollut. R 28:936–946.

Wang, X., W. Liu, G. Jin, Z. Wu, D. Zhang, Y. Bao, and W. Shi. 2022. Salvia miltiorrhiza polysaccharides alleviates florfenicol induced kidney injury in chicks via inhibiting oxidative stress and apoptosis. Ecotoxicol. Environ. Saf. 233:113339.

Wang, X. Y., Y. An, W. Y. Jiao, Z. Y. Zhang, H. Han, X. H. Gu, and X. H. Teng. 2018b. Selenium protects against lead-induced apoptosis via endoplasmic reticulum stress in chicken kidneys. Biol. Trace Element Res. 182:354–363.

Wang, Y., H. Zhao, M. Guo, Y. Shao, J. Liu, G. Jiang, and M. Xing. 2018c. Arsenite renal apoptotic effects in chickens co-aggravated by oxidative stress and inflammatory response. Metallomics: Integ. Biometal Sci. 10:1805–1813.

Yao, T., L. Zhang, Y. Fu, L. Yao, C. Zhou, and G. Chen. 2021. Saikosaponin-d alleviates renal inflammation and cell apoptosis in a mouse model of sepsis via TCF7/FOSL1/matrix metalloproteinase 9 inhibition. Mol. Cell. Biol. 41:e0033221.

Yu, S., H. Ji, X. Dong, A. Liu, and J. Yu. 2020. FAS/FAS-L-mediated apoptosis and autophagy of SPC-A-1 cells induced by water-soluble polysaccharide from Polygala tenuifolia. Int. J. Biol. Macromol. 150:449–458.

Zhang, J., J. Cui, Y. Wang, X. Lin, X. Teng, and Y. Tang. 2022. Complex molecular mechanism of ammonia-induced apoptosis in chicken peripheral blood lymphocytes: miR-27b-3p, heat shock proteins, immunosuppression, death receptor pathway, and mitochondrial pathway. Ecotoxicol. Environ. Saf. 236: 113471.

Zhang, Q., C. Liu, Q. Li, J. Li, Y. Wu, and J. Liu. 2019. MicroRNA-25-5p counteracts oxidized LDL-induced pathological changes by targeting neuronal growth regulator 1 (NEGR1) in human brain micro-vessel endothelial cells. Biochimie 165:141–149.